

E1-2016-54

Ts. Baatar<sup>1</sup>, B. Batgerel<sup>1</sup>, A. I. Malakhov, R. Togoo<sup>1</sup>,  
G. Sharkhuu<sup>1</sup>, B. Otgongerel<sup>1</sup>, T. Tulgaa<sup>1</sup>

THERMODYNAMIC CHARACTERISTICS  
OF THE SECONDARY PARTICLES PRODUCED  
IN  $\pi^-$ -C INTERACTIONS AT 40 GeV/c AS A FUNCTION  
OF CUMULATIVE NUMBER  $n_c$

Submitted to "Physics of Atomic Nuclei"

---

<sup>1</sup>Institute of Physics and Technology, Mongolian Academy of Sciences,  
Ulaanbaatar

Баатар Ц. и др.

E1-2016-54

Термодинамические характеристики вторичных частиц, рожденных в  $\pi^-C$  взаимодействиях при импульсе 40 ГэВ/с, как функция кумулятивного числа  $n_c$

Рассматриваются множественные процессы рождения частиц в  $\pi^-C$  взаимодействиях при импульсе 40 ГэВ/нуклон по кумулятивному числу  $n_c$ . Локальные значения температуры, давления, объема и плотности энергии в области взаимодействия определяются как функция кумулятивного числа. Этот анализ дает возможность изучать пространственно-временную картину и процесс фазового перехода при высоких энергиях.

Работа выполнена в Лаборатории физики высоких энергий им. В. И. Векслера и А. М. Балдина ОИЯИ.

Препринт Объединенного института ядерных исследований. Дубна, 2016

Baatar Ts. et al.

E1-2016-54

Thermodynamic Characteristics of the Secondary Particles Produced in  $\pi^-C$  Interactions at 40 GeV/c as a Function of Cumulative Number  $n_c$

The multiparticle production process in  $\pi^-C$  interactions at 40 GeV/c has been studied on cumulative number  $n_c$ . Local values of temperature, pressure, volume, and energy density in the interaction region are determined as a function of the cumulative number. This analysis gives us an opportunity of studying a space-time picture and the phase transition process at high energies.

The investigation has been performed at the Veksler and Baldin Laboratory of High Energy Physics, JINR.

Preprint of the Joint Institute for Nuclear Research. Dubna, 2016

## INTRODUCTION

The investigation of the multiparticle production process in hadron–nucleus ( $hA$ ) and nucleus–nucleus ( $AA$ ) interactions at high energies and large momentum transfers plays a very important role for understanding the strong interaction mechanism and inner quark–gluon structure of the nuclear matter.

According to the fundamental theory of the strong interaction, QCD [1], the interactions between quarks and gluons become weaker as the exchange momentum increases. Consequently, at large temperatures/densities, the interactions which confine quarks and gluons inside hadrons should become sufficiently weak to release them [2].

It is expected that the QCD phase transition processes may be realized in  $hA$  and  $AA$  interactions at high energies and large momentum transfers, in other words, these interactions give us an opportunity to study the nuclear matter under extreme conditions.

Over the recent years the collective phenomena such as the cumulative particle production [3], the production of nuclear matter with high densities, the phase transition from the hadronic matter to the quark–gluon plasma state, and color-superconductivity are widely discussed in the literature [3–7].

In  $hA$  and  $AA$  interactions, in contrast to  $hN$  interactions, secondary particles may be produced as a result of multinucleon interactions, in other words, the particles are produced in the region kinematically forbidden for  $hN$  interactions.

According to different ideas and models, if these phenomena exist in the nature, then they will be observed in the above-mentioned reactions and should influence the dynamics of the interaction process, and they will be reflected in the angular and momentum characteristics of the reaction products.

In this paper, we consider the following reactions:

$$\pi^- + C \rightarrow p + X, \quad (1)$$

$$\pi^- + C \rightarrow \pi^- + X \quad (2)$$

at 40 GeV/ $c$ . This paper is the continuation of our previous publications [4, 8]. 8791  $\pi^-C$  interactions have been used in this analysis. 12441 protons and 30145  $\pi^-$  mesons have been detected in these interactions.

## 1. EXPERIMENTAL METHOD

The experimental material was obtained by means of the Dubna two-meter propane (C<sub>3</sub>H<sub>8</sub>) bubble chamber exposed to  $\pi^-$  mesons with a momentum of 40 GeV/c from Serpukhov accelerator. All distributions in this paper have been obtained under conditions of  $4\pi$  geometry.

The average error of the momentum measurements is  $\sim 12\%$ , and the average error of the angular measurements is  $\sim 0.6\%$ .

All secondary negative particles are taken as  $\pi^-$  mesons. The average boundary momentum from which  $\pi^-$  mesons were well identified in the propane bubble chamber is  $\sim 70$  MeV/c. In connection with the identification problem between energetic protons and  $\pi^+$  mesons, the protons with a momentum more than  $\sim 1$  GeV/c are included into  $\pi^+$  mesons. The average boundary momentum from which protons are detected in this experiment is  $\sim 150$  MeV/c. So, the secondary protons with momentum from  $\sim 150$  MeV/c to  $\sim 1$  GeV/c are used for proton distributions.

## 2. TEMPERATURE $T$ AS A FUNCTION OF VARIABLE $n_c$

In our previous paper [4], we studied the dependences of the temperature  $T$  on the variable  $n_c$  (or  $t$ ), called the cumulative number. This variable  $n_c$  in the fixed target experiment is determined by the following formula:

$$n_c = \frac{(P_a \cdot P_i)}{(P_a \cdot P_b)} = \frac{E_i - \beta_a \cdot P_i^{II}}{m_p} \cong \frac{E_i - P_i^{II}}{m_p}. \quad (3)$$

Here  $P_a$ ,  $P_b$ , and  $P_i$  are the four-dimensional momenta of the incident particle, target, and the considered secondary particles, correspondingly;  $E_i$  is the energy and  $P_i^{II}$  is the longitudinal momentum of the secondary particles;  $\beta_a = \frac{P_a}{E_a}$  is the velocity of the incident particle. At high-energy experiment  $\beta_a \cong 1$ , so it may be omitted,  $m_p$  is the proton mass. From formula (3) we see that this variable is relativistic invariant.

On the other hand, the variable  $n_c$  at high energies is related with the momentum transfer  $t$  by the following formula:

$$t = 2E_a \cdot m_p \left( \frac{E_i - \beta_a P_i^{II}}{m_p} \right) \cong S_{hN} \cdot n_c, \quad (4)$$

where  $S_{hN} = 2E_a m_p$  is the total energy square for  $hN$  interaction, which is constant in every experiment, so  $n_c$  may be used as the main variable.

For the secondary particles produced in the region kinematically forbidden for  $hN$  interactions, this variable  $n_c$  takes the value more than 1, i.e.,  $n_c > 1$ .

This fact gives us an opportunity to know which particles in the given event are produced in the region not allowed for  $hN$  interaction. This is another reason why we have used this variable.

The transverse energy spectrum of the secondary particles produced in  $hA$  and  $AA$  interactions at high energies may reflect the dynamics of the interaction process more clearly. This is related with the fact that the transverse effects are mainly generated during the interaction process.

The effective temperature  $T$  of the secondary protons from reaction (1) as a function of the variable  $n_c$  is presented in Fig. 1 [4].

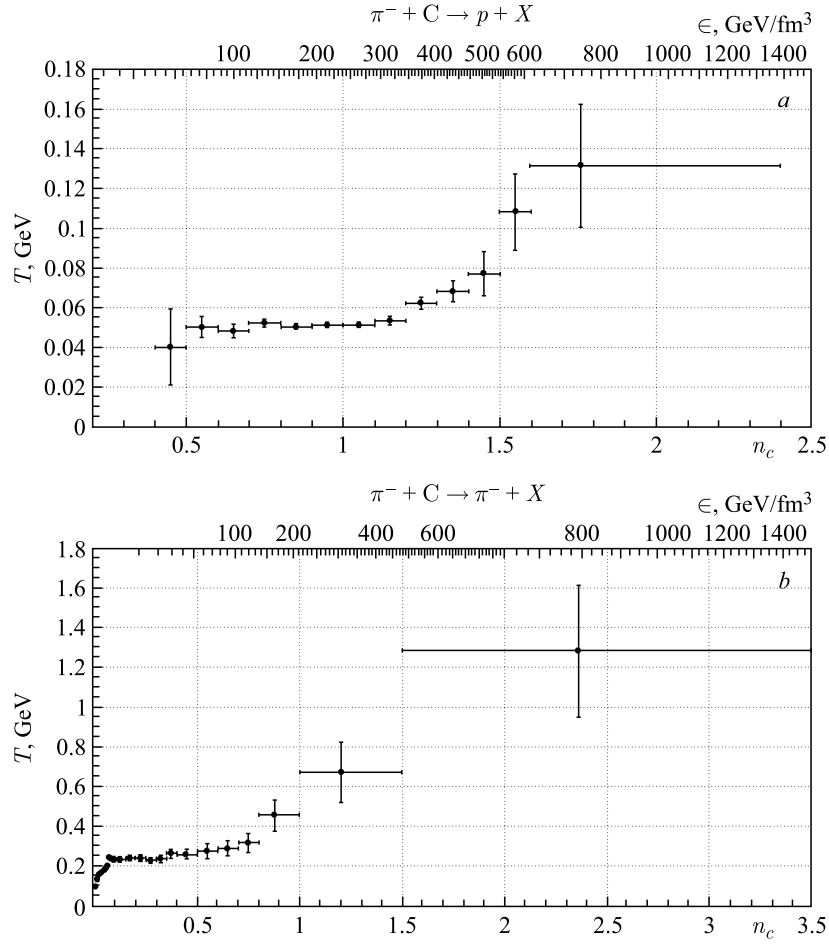


Fig. 1. Dependence of the effective temperature  $T$  on the variable  $n_c$  for the secondary protons (a) and the secondary  $\pi^-$  mesons (b)

From Fig. 1, *a* we see that the effective temperature  $T$  remained practically constant at the level of  $T \cong 50$  MeV until  $n_c \cong 1.2$  and then increases. We note that there are no experimental points in  $n_c < 0.4$  region. This is related with complications to identify protons with momentum  $P_p > 1$  GeV/ $c$  from energetic  $\pi^+$  mesons.

The similar dependence for  $\pi^-$  mesons from reaction (2) is presented in Fig. 1, *b*. From this figure we see that with increasing  $n_c$  the effective temperature  $T$  in the beginning is increasing until  $n_c \cong 0.07$ , and then in the  $0.07 < n_c < 0.5$  interval the temperature  $T$  remains practically constant at the level of  $T \cong 0.234$  GeV and then essentially increases.

Strong changing of the dependences of temperature  $T$  on the variable  $n_c$  may be an indication of another mechanism of particle production in these regions. If so, the first region with increasing  $T$  until  $T \cong 200$  MeV and  $n_c \leq 0.07$  may correspond to the thermalization of the interacting objects (here the strongly interacting matter is in the thermally excited hadronic phase); the second region with approximately constant  $T_c \cong 234$  MeV in the  $0.07 \leq n_c \leq 0.5$  region for  $\pi^-$  mesons and with constant  $T_c \cong 50$  MeV in the  $0.5 \leq n_c \leq 1.2$  region for protons may be an indication of the equilibrium state formation (hadron + quarks, gluons); and the third region, which shows the significant increasing of the temperature  $T$  in  $n_c > 0.5$  for  $\pi^-$  mesons and  $n_c > 1.2$  for protons, can be related with the production of pure QGP state.

Our results have shown that the locations of the transition lines, temperatures in the QGP states of the phase transition processes for protons and pions are different.

### 3. DEPENDENCE OF VOLUME AND ENERGY DENSITY ON VARIABLE $n_c$

The dependence of the energy density on the variable  $n_c$  may be determined by the following formula:

$$\epsilon(n_c) = \frac{\sqrt{S_{hN} \cdot n_c}}{V(n_c)}, \quad (5)$$

where  $\sqrt{S_{hN} \cdot n_c}$  is the energy for producing the secondary particles at given  $n_c$  and  $V(n_c)$  is the corresponding volume.

We would like to note that at summarizing the formula (3) by all secondary particles produced in the event, we obtain the value of the total energy square determined on the basis of the energy–momentum conservation law, i.e.:

$$Q^2 = S_{hN} \cdot M_t = S_{hN} \cdot \sum_{i=1}^n \frac{(E_i - \beta_a P_i^{II})}{m_p}, \quad Q^2 \rightarrow S. \quad (6)$$

We see that this formula is additive. If we detect all secondary particles produced in the event, then the total transferred momentum  $Q^2$  determined by

all secondary particles tends to the total energy square  $S$ . This allows us to use formula (4) to estimate the energy density.

Now we will consider the case of the dependence of the volume on  $n_c$ . To do this, we have used our previous result on the particle emission region size,  $r$  [8]. This characteristic length  $r$  at high energies is determined by the formula:

$$r = \frac{1}{m_p \sqrt{n_c}} = \lambda_c^p = \frac{0.21 \text{ fm}}{\sqrt{n_c}}. \quad (7)$$

We see that parameter  $r$  is inverse proportional to the variable  $n_c$ . Here  $\lambda_c^p = 0.21 \text{ fm}$  is the Compton wave length of the proton. We also see that the secondary particles are produced at  $n_c = 1$ , the parameter  $r$  is equal to  $\lambda_c^p$  ( $r = \lambda_c^p = 0.21 \text{ fm}$ ), and if  $n_c < 1$ , then  $r > \lambda_c^p$ , and if  $n_c > 1$  (for cumulative particles), then  $r < \lambda_c^p$ . In this case the time scale can be determined as  $\Delta t = \frac{r[\text{fm}]}{c}$ .

Now we have an opportunity to determine the local  $V(n_c)$  from which the particle is emitted. In the first approximation  $V(n_c)$  is regarded as a spherical bubble with the parameter  $r$  calculated by the formula (7):

$$V(n_c) = \frac{4\pi}{3} r^3 = \frac{4\pi}{3} \cdot \frac{(0.21)^3}{n_c^{3/2}} [\text{fm}^3]. \quad (8)$$

The dependence of the volume  $V$  on the variable  $n_c$  is shown in Fig. 2. Experimental points for protons (black circles) and  $\pi^-$  mesons (open triangles) from

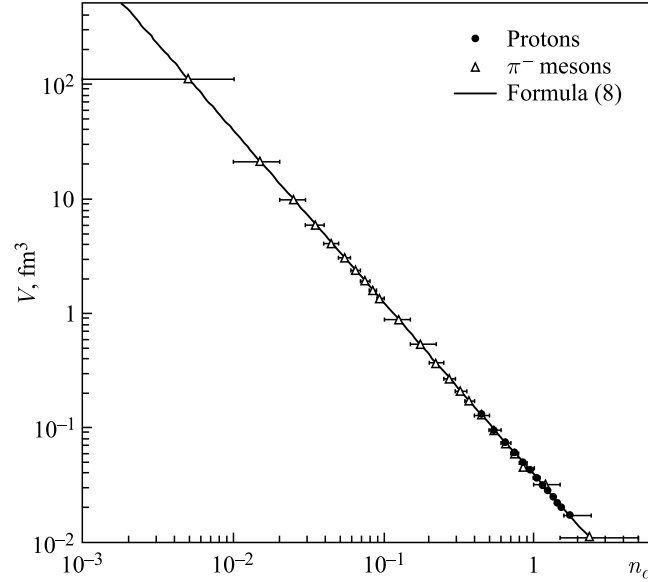


Fig. 2. Dependence of the volume  $V$  on the variable  $n_c$

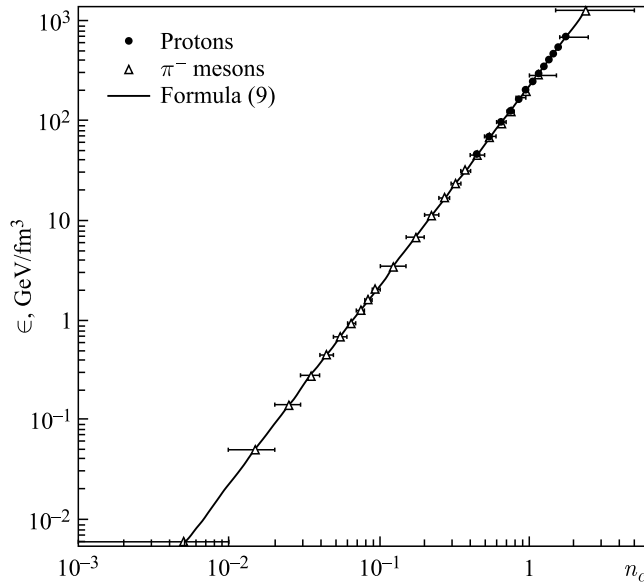


Fig. 3. Energy density  $\epsilon$  as a function of the variable  $n_c$

$\pi^-$ -C interactions at 40 GeV/c calculated by formula (8) are also shown in this figure. We see that while the variable  $n_c$  is increasing the volume  $V$  is decreasing.

After determining the local volume  $V(n_c)$ , we can calculate the local energy density  $\epsilon(n_c)$  using formulae (8) and (5):

$$\epsilon(n_c) = \frac{\sqrt{S_{hN}} n_c^2}{\frac{4\pi}{3} (0.21)^3} \frac{\text{GeV}}{\text{fm}^3}. \quad (9)$$

This dependence is shown in Fig.3. Experimental values for protons (black circles) and  $\pi^-$  mesons (open triangles) calculated by formula (9) are also shown in this figure. This dependence shows that with increasing  $n_c$  the energy density  $\epsilon$  is essentially increasing.

From formula (9) we see that the local energy density  $\epsilon(n_c)$  is determined by  $\sqrt{S_{hN}}$  and  $n_c^2$ , in other words, by means of experimentally measurable quantities without model-dependent assumptions. This is, of course, the main advantage of this formula.

So, we have obtained the local energy density  $\epsilon(n_c)$  and volume  $V(n_c)$ .

Now we will consider the case of the pressure  $P(n_c)$ . To do this, we have used the Clapeyron equation for the ideal gas. This equation gives the relation between pressure  $P$ , volume  $V$ , and temperature  $T$  and can be written in the following form:

$$P(n_c) \cdot V(n_c) = k_B T(n_c). \quad (10)$$

Using this formula, we can determine pressure  $P(n_c)$ :

$$P(n_c) = \frac{k_B T(n_c)}{V(n_c)} = \frac{k_B T(n_c) \cdot n_c^{3/2}}{\frac{4\pi}{3}(0.21)^3} \frac{\text{GeV}}{\text{fm}^3}. \quad (10')$$

The pressure  $P(n_c)$  as a function of variable  $n_c$  is shown in Fig. 4. We see that with increasing  $n_c$  the pressure  $P(n_c)$  increases, and at large values of the variable  $n_c$  the pressure increases more rapidly.

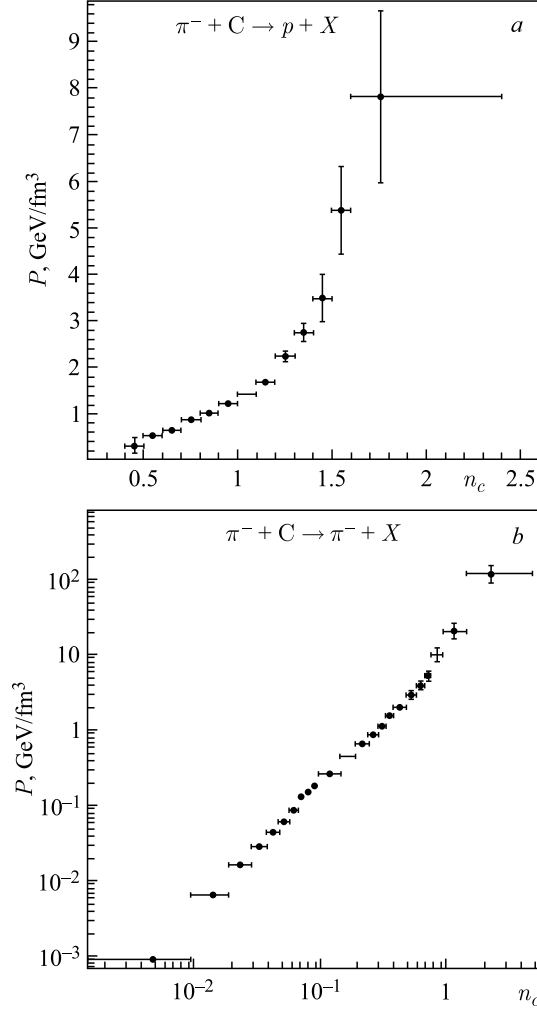


Fig. 4. Dependence of the pressure  $P(n_c)$  on the variable  $n_c$  for protons (a) and  $\pi^-$  mesons (b)

The dependence between the pressure  $P(n_c)$  and the temperature  $T(n_c)$  is presented in Figs. 5, *a, b*. This dependence is called a curve of equilibrium of phases.

From Fig. 5, *b* we see that with increasing  $T(n_c)$  the pressure  $P(n_c)$  increases until  $T = 0.200$  GeV, and then the temperature  $T$  remains practically constant at the level of  $T = 0.234$  GeV, while the pressure  $P(n_c)$  increases monotonously from  $P_c^1(n_c) \cong 127.1$  GeV/fm<sup>3</sup> to  $P_c^2(n_c) \cong 1113.4$  GeV/fm<sup>3</sup>, and then with

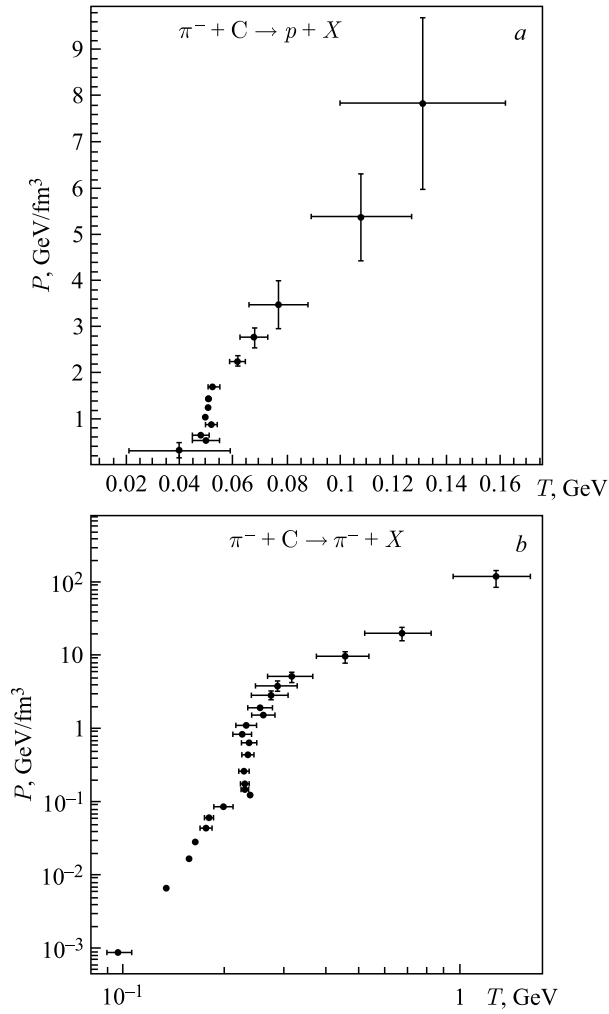


Fig. 5. Dependence between the pressure  $P$  and the temperature  $T$  for protons (*a*) and  $\pi^-$  mesons (*b*)

further increasing of  $T$ , the pressure rises again. So, we can conclude that in the pressure interval  $P_c^1 \leq P \leq P_c^2$  with practically constant  $T \cong 0.234$  GeV the equilibrium state (or mixed phase) is established.

The region with  $T \leq T_c \cong 0.234$  GeV and  $P \leq P_c^1 = 127.1$  GeV/fm<sup>3</sup> belongs to the thermally excited hadronic phase, and the region with  $T > T_c \cong 0.234$  GeV and  $P > P_c^2 = 1113.4$  GeV/fm<sup>3</sup> belongs to the QGP state.

In the case of the secondary protons the similar dependence between  $P$  and  $T$  is observed (Fig. 5). The thermal equilibrium state is established at  $T_c \cong 50$  MeV in contrast to the  $\pi^-$  meson case. So, the region with  $T_c = 50$  MeV and pressure interval  $P_c^1 \cong 526.0$  GeV/fm<sup>3</sup>  $\leq P \leq P_c^2 \cong 1685.7$  GeV/fm<sup>3</sup> belongs to the thermal equilibrium state, and the region with  $T > T_c \cong 50$  MeV and  $P > P_c^2 \cong 1685$  GeV/fm<sup>3</sup> corresponds to the QGP state for protons.

We note that due to the identification problem of protons with momentum  $P > 1$  GeV/c we have no experimental points in the region with  $T < T_c \cong 50$  MeV and  $P < P_c^1 = 526$  GeV/fm<sup>3</sup>.

We also note that at increasing the temperature  $T$  the pressure  $P(n_c)$  increases and the volume  $V(n_c)$  decreases. So, at establishing the equilibrium the two effects are mutually compensating each other for both cases of protons and  $\pi^-$  mesons from  $\pi^-$ C interactions at 40 GeV/c.

Finally, we would like to stress that the dependence of the pressure  $P$  on the temperature  $T$  is, of course, the consequence of the dependence of the temperature  $T$  on the variable  $n_c$ , but it gives us additional information on the critical pressures  $P_c^1$  and  $P_c^2$ .

## CONCLUSIONS

In this paper, we have determined the local energy density  $\epsilon(n_c)$ , temperature  $T(n_c)$ , pressure  $P(T, n_c)$ , and volume  $V(n_c)$  of the interaction region. This gives us an opportunity to study the space-time picture of the multiparticle production process at high energies including the phase transition from the hadronic state to the quark–gluon plasma.

## REFERENCES

1. Gross D. J., Wilczek F. // Phys. Rev. Lett. 1973. V. 30. P. 1343; Politzer H. D. // Ibid. P. 1346.
2. Collins J. C., Perry M. J. // Phys. Rev. Lett. 1975. V. 34. P. 1353.
3. Baldin A. M. // Part. Nucl. 1977. V. 8. P. 429.
4. Baatar Ts. et al. // Proc. of XXI Intern. Baldin Seminar on High Energy Physics Problems, JINR, Dubna, Russia, Sept. 10–15, 2012. Dubna, 2013.

5. *Rajagopal K., Wilczek F.* hep-ph/0011333. 2000.
6. *Rischke Dirk H.* arXiv:nucl-th/0305030v2.
7. *Hagedorn R.* // *Nouvo Cim. Suppl.* 1965. V. 3. P. 147.
8. *Baatar Ts. et al.* // *Proc. of XXII Intern. Baldin Seminar on High Energy Physics Problems, Dubna, Russia, Sept. 15–20, 2014.*

Received on July 27, 2016.

Редактор *Е. И. Крупко*

Подписано в печать 24.08.2016.

Формат 60 × 90/16. Бумага офсетная. Печать офсетная.

Усл. печ. л. 0,75. Уч.-изд. л. 0,72. Тираж 255 экз. Заказ № 58889.

Издательский отдел Объединенного института ядерных исследований  
141980, г. Дубна, Московская обл., ул. Жолио-Кюри, 6.

E-mail: [publish@jinr.ru](mailto:publish@jinr.ru)

[www.jinr.ru/publish/](http://www.jinr.ru/publish/)